

On the Performance of RIS-Enhanced RSMA Networks with On-Off Control

Haiyan Huang^{1,*}, Dongjie Jiang¹, Nina Zhang², Linlin Liang³ and Hongyan Zhang¹

¹School of Electronics and Information Engineering, Lanzhou Jiaotong University, Lanzhou Gansu 730070, China

²Shaanxi General Staff of PAP, Xi'an Shaanxi 710054, China

³School of Network and Information Security, Xidian University, Xi'an Shaanxi 710071, China

Abstract

As a pivotal enabling technology for the 6G wireless communication system, Reconfigurable intelligent surface (RIS) is capable of dynamically adjusting its electromagnetic elements, thereby significantly enhancing wireless network coverage, spectral efficiency, and energy sustainability. In this context, this paper investigates the integration of RIS into the rate-splitting multiple access (RSMA) framework, where the base station employs the RIS to transmit superimposed signals to multiple users simultaneously. To reduce computational complexity, a On-Off control scheme is adopted, considering both imperfect successive interference cancellation (ipSIC) and perfect successive interference cancellation (pSIC) scenarios. Closed-form expressions for the exact outage probability of the k -th user under Rayleigh fading channels are derived. Furthermore, to more comprehensively evaluate system performance, asymptotic outage probability expressions for ipSIC/pSIC in the high signal-to-noise ratio (SNR) regime are also derived. The results demonstrate that, under identical system configurations, the RSMA-based communication scheme outperforms the non-orthogonal multiple access (NOMA) scheme, exhibiting superior spectral resource utilization and interference management capabilities. In the pSIC scenario, the user diversity order is contingent upon the number of RIS reflecting elements and the channel ordering approach. Increasing the number of RIS reflecting elements can effectively compensate for the performance degradation caused by residual interference in the ipSIC scenario, thereby further enhancing system performance.

Received on 30 June 2024; accepted on 25 August 2024; published on 11 June 2025

Keywords: Reconfigurable Intelligent Surface, Rate-Splitting Multiple Access, Imperfect SIC, On-Off Control

Copyright © 2025 H. Huang *et al.*, licensed to EAI. This is an open access article distributed under the terms of the Creative Commons Attribution license (<http://creativecommons.org/licenses/by/4.0/>), which permits unlimited use, distribution and reproduction in any medium so long as the original work is properly cited.

doi:10.4108/eetsis.9518

1. Introduction

With the rapid development of wireless communication technologies, the demand for spectral efficiency and network capacity has been increasing continuously [1]. To address this challenge, Reconfigurable intelligent surfaces (RIS), as a revolutionary technology, have attracted widespread attention due to their ability to intelligently manipulate the wireless propagation environment [2]. RIS is a planar structure composed of a large number of programmable reflecting elements. These elements can intelligently adjust the phase, amplitude, and polarization of wireless signals, enabling real-time adjustment of the RIS reflection

pattern to reduce signal attenuation and interference, thereby enhancing the spectral efficiency and network capacity of the system. Meanwhile, rate-splitting multiple access (RSMA), as a generalized multiple access technology, has been recognized as a promising multiple access technology for 6G wireless communications due to its outstanding capabilities in improving spectral efficiency and user fairness [3]. RSMA bridges the two extreme interference management strategies of fully decoding interference and treating interference as noise by splitting user messages and enabling non-orthogonal transmission of common messages and user-specific private messages [4].

In recent years, researchers have explored the integration of RIS-assisted communication systems with RSMA protocols. The authors of [5] analyzed

*Corresponding author. Email: huanghaiyan@mail.lzjtu.cn

the outage performance of RIS-assisted downlink non-orthogonal multiple access (NOMA) systems. Considering user utilization rates, the authors in [6] analyzed discrete phase-shift RIS reflections for RIS-assisted NOMA and orthogonal multiple access (OMA). In scenarios involving user ordering, joint optimization of beamforming vectors and phase-shift matrices was conducted to reduce transmit power [7]. Taking into account imperfect successive interference cancellation in non-orthogonal multiple access communications [8], the authors analyzed the system's outage performance. The authors of [9] designed a low-complexity resource allocation scheme for RIS-assisted uplink RSMA systems, significantly improving the maximum transmission delay. In [10], an RSMA communication system for RIS-assisted cell-edge users and nearby users was analyzed, where outage probability expressions were derived considering phase-shift-based switching techniques. Z. Yang et al. considered energy efficiency maximization for RIS-assisted RSMA communications by jointly optimizing RIS phase shifts and base station (BS) beamforming [11].

It is worth noting that while [5] provides an outage probability analysis for RIS-assisted NOMA systems, a similar analysis for RSMA has not yet been addressed. Additionally, [6] considers discrete phase shifts in RIS-assisted NOMA and OMA systems, and [8] investigates imperfect successive interference cancellation in NOMA systems, but the analysis for RSMA systems remains to be conducted. Although [10] considers RIS-assisted RSMA networks, it omits the mathematical framework for discrete phase shifts.

Based on the above analysis, this paper investigates RIS-assisted RSMA communication systems. By considering discrete phase shifts of RIS, user utilization rates, and user ordering, we derive the outage probability expressions for the system and analyze the impact of imperfect successive interference cancellation and discrete phase shifts of RIS on the outage performance of the communication system.

2. System Model

According to the illustration in Fig. 1, the RIS-assisted RSMA communication model consists of three parts, including a BS, RIS, and K end users. It is assumed that each of the BS and users is endowed with a single antenna, where BS sends signals to K end users through the use of RIS. RIS is furnished with N reflection units, which are controllable through software focused on communication functionality. The complex channel coefficients for the BS-RIS link, as well as the RIS-users link, are expressed by h_i and g_{ik} respectively. Both h_i and g_{ik} follow the complex Gaussian distribution with the mean set to zero and the variance specified

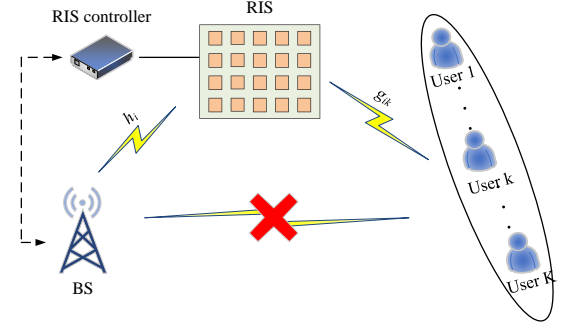


Figure 1. RIS-assisted downlink RSMA network model.

as σ^2 and are independent of each other. Given that the BS-users link is obstructed by tall buildings, resulting in a lack of direct interconnection, the communication channel between any two nodes within this environment is characterized by the Rayleigh fading model. The background noise of these wireless links is additive white Gaussian noise, with statistical properties including a mean of zero and a variance of N_0 .

The communication system assumes that the channel state information, the geographic coordinates of the BS, and the seamless feedback to the RIS can be implemented accurately. In order to facilitate the analysis, the effective cascade channel gain of the BS-RIS-user link is sorted: $|g_{i1}^H \Phi h_i|^2 \leq \dots \leq |g_{ik}^H \Phi h_i|^2 \leq \dots \leq |g_{iK}^H \Phi h_i|^2$, where $\Phi = \text{diag}(\beta e^{-j\theta_1}, \dots, \beta e^{-j\theta_i}, \dots, \beta e^{-j\theta_K})$ represents the phase shift matrix of RIS, and $\beta \in [0, 1]$ and $\theta_i \in [0, 2\pi)$ represent the fixed reflection amplitude and phase shift parameter of the k -th reflection unit of RIS, respectively. Without loss of generality, it is assumed that when the RIS is not within the frequency band, that is, the incident frequency does not fall within the designed unit's response band, the RIS is basically total reflection.

In the communication process, BS uses the RSMA protocol, and the superimposed signal sent to the end user includes a public message x_c and K mutually orthogonal private information x_k , $\{k \in 1, 2, \dots, K\}$ represents K different users. As a result, the signal that receives at the k -th user after RIS reflection is:

$$y_k = (g_{ik}^H \Phi h_i) \left(\sqrt{\alpha_c P_B} x_c + \sum_{i=1}^K \sqrt{\alpha_i P_B} x_i \right) + w_k \quad (1)$$

where P_B is the transmission power of the BS, α_c and α_i are the rate splitting factors of the base station sending public information and private information respectively. In order to meet the user fairness, the rate splitting factors of the public information and the k th user satisfy the relationship $\alpha_c + \sum_{i=1}^K \alpha_i = 1$, and

$\alpha_c \geq \alpha_1 \geq \dots \geq \alpha_k \geq \dots \geq \alpha_K$. x_c, x_i represent the public information sent and the private information of K users respectively, and $E\{x_c^2\} = E\{x_i^2\} = 1$. w_k are additive Gaussian white noise with mean value of 0 and variance N_0 .

After receiving the superimposed signal sent by BS, user U_k first decodes the public message x_c , and then decodes his own private message x_k after deleting the public message x_c by SIC. When decoding x_c , all private messages will cause interference, and when x_k is decoded, the private information of other users will cause interference. Therefore, the SNR of U_k decoding public message and private messages can be expressed:

$$\gamma_k^c = \frac{\alpha_c P_B |g_{ik}^H \Phi h_i|^2}{\sum_{i=1}^K \alpha_i P_B |g_{ik}^H \Phi h_i|^2 + N_0} \quad (2)$$

$$\gamma_k^p = \frac{\alpha_k P_B |g_{ik}^H \Phi h_i|^2}{\sum_{\substack{i=1 \\ i \neq k}}^K \alpha_i P_B |g_{ik}^H \Phi h_i|^2 + \omega P_B |h_{irru}|^2 + N_0} \quad (3)$$

where $\omega \in [0, 1]$ is the imperfect successive interference cancellation coefficient, $\omega = 0$ denotes ipSIC and $\omega = 1$ denotes pSIC.

For the convenience of analysis, Assuming the residual interference arising from the implementation of ipSIC follows a Rayleigh fading model, and the corresponding complex channel parameter is represented by h_{irru} , which obeys the complex Gaussian distribution with mean 0 and variance σ_{irru}^2 . In addition, in order to facilitate the next calculation, the probability density function(PDF) of $|h_{irru}|^2$ is:

$$f_{|h_{irru}|^2}(y) = \frac{1}{\sigma_{irru}^2} e^{-\frac{y}{\sigma_{irru}^2}} \quad (4)$$

3. On-Off Control Scheme

Considering that in the actual communication scenario, constantly changing the reflection elements of RIS to adjust and control the amplitude and phase of the signal is conducive to improving the performance of the network. However, this alternative requires precise design specifications, as well as an expensive hardware configuration, which will lead to the cost of RIS becoming higher. For the sake of convenient analysis and implementation, a low-cost implementation is to apply switch control to the RIS-RSMA network to realize the amplitude and phase shift level of the RIS-assisted RSMA network[12], that is, each diagonal element in the phase shift matrix Φ is either 0 (off) or 1 (on). Meanwhile, increasing the number of reflection units remains a scalable and cost-effective solution.

RIS has N reflection units. Suppose $N = LQ$, where L and Q are both integers. Let $\Psi = \frac{1}{\sqrt{Q}} I_L \otimes \mathbf{1}_Q$, where I_L is the unit matrix of $L \times L$, $\mathbf{1}_Q$ is the 1-vector of $Q \times 1$, Ψ_l denotes the l column of Ψ , and for $l \neq p$, $\Psi_l^H \Psi_p = 0$, $\Psi_l^H \Psi_l = 1$. Using On-Off control, a random column of Ψ_l can be selected to maximize the SNR of user U_k decoding. (2) and (3) can be rewritten as:

$$\tilde{\gamma}_k^c = \max_{\Psi_l} \frac{\alpha_c P_B |\Psi_l^H D_k h_i|^2}{\sum_{i=1}^K \alpha_i P_B |\Psi_l^H D_k h_i|^2 + N_0} \quad (5)$$

$$\tilde{\gamma}_k^p = \max_{\Psi_l} \frac{\alpha_k P_B |\Psi_l^H D_k h_i|^2}{\sum_{\substack{i=1 \\ i \neq k}}^K \alpha_i P_B |\Psi_l^H D_k h_i|^2 + \omega P_B |h_{irru}|^2 + N_0} \quad (6)$$

where D_k is a diagonal matrix whose diagonal elements are obtained by g_{ik} .

Theorem 1. In order to simplify the analysis of the outage performance of the system, the cascade channel gain of the RIS aided link is expressed as $|Z|^2 = |\Psi_l^H D_k h_i|^2$ by using the On-Off control scheme. At this point, the cumulative distribution function(CDF) of $|Z|^2$ can be written as:

$$F_{|Z|^2}(z) = \mu \sum_{b=0}^{K-k} \binom{K-k}{b} \frac{(-1)^b}{k+b} \times \left[1 - \frac{2}{\Gamma(Q)} \left(\frac{\sqrt{z}}{\sigma^2} \right)^Q K_Q \left(\frac{2\sqrt{z}}{\sigma^2} \right) \right]^{k+b} \quad (7)$$

where $\mu = \frac{K!}{(K-k)!(k-1)!}$.

Proof. See Appendix A. ■

4. Performance Analysis

In wireless communication, outage probability is an important performance metric to measure the reliability of communication links under certain conditions. The outage performance refers to the probability that the communication link is interrupted within a given period of time, which is contingent upon the mean SNR of the communication link, along with the specific model that characterizes its channel fading distribution

4.1. Exact Outage Probability of the RSMA Scheme

According to the principle of RSMA, there are two cases in the RIS-assisted RSMA communication network that may cause communication interruption: (1) U_k cannot successfully decode the public information x_c after BS sends the superimposed signal; (2) U_k successfully

decodes public information x_c , but cannot successfully decode its own private information x_k . Therefore, the outage probability of user U_k is defined as:

$$\begin{aligned} OP &= \Pr(\tilde{\gamma}_k^c < \gamma_{thc}) + \Pr(\tilde{\gamma}_k^c > \gamma_{thc}, \tilde{\gamma}_k^p < \gamma_{thp}) \\ &= 1 - \Pr(\tilde{\gamma}_k^c > \gamma_{thc}, \tilde{\gamma}_k^p > \gamma_{thp}) \end{aligned} \quad (8)$$

where $\gamma_{thc} = 2^{R_c} - 1$ and $\gamma_{thp} = 2^{R_p} - 1$ are the threshold SNRs for the transmission of public and private messages, respectively, R_c and R_p are the target data rates at which they decode the messages, respectively. $\Pr(\cdot, \cdot)$ denotes the joint probability. By the concept of joint probability in [13], the outage probability of (8) can be further simplified as:

$$OP = F_{\tilde{\gamma}_k^c}(\gamma_{thc}) + F_{\tilde{\gamma}_k^p}(\gamma_{thp}) - F_{\tilde{\gamma}_k^c, \tilde{\gamma}_k^p}(\gamma_{thc}, \gamma_{thp}) \quad (9)$$

where $F_X(\cdot)$ is the cumulative distribution function of the variable X , and $F_{X,Y}(\cdot, \cdot)$ is the joint CDF of X and Y .

In the realm of wireless communication, attaining pSIC is often considered an idealized scenario. However, in practical communication settings, achieving such perfection becomes challenging due to various factors, including hardware limitations, channel estimation errors, and signal processing constraints. In the subsequent analysis, we provide outage probability expressions for both perfect SIC and imperfect SIC scenarios. Furthermore, in the following chapter, these two cases will be simulated and verified accordingly.

4.1.1 Imperfect SIC. Using the On-Off control scheme, and considering the existence of imperfect SIC to generate residual interference, Eq.(9) can be rewritten as:

$$\begin{aligned} OP &= \prod_{l=1}^L F_{|Z|^2}(\tau_c) + \prod_{l=1}^L F_{|Z|^2}((\omega P_B |h_{irul}|^2 + N_0) \tau_p) \\ &\quad - \prod_{l=1}^L F_{|Z|^2}(\min\{\tau_c, (\omega P_B |h_{irul}|^2 + N_0) \tau_p\}) \end{aligned} \quad (10)$$

$$\text{where } \tau_c = \frac{\gamma_{thc} N_0}{\left(\alpha_c - \sum_{i=1}^K \alpha_i \gamma_{thc}\right) P_B}, \quad \tau_p = \frac{\gamma_{thp}}{\left(\alpha_k - \gamma_{thp} \sum_{i=1, i \neq k}^K \alpha_i\right) P_B}$$

In order to facilitate analysis and implementation, assuming that the marginal and joint statistics of $\tilde{\gamma}_k^c$ and $\tilde{\gamma}_k^p$ are the same for all l [10], the outage probability of (9) can be further written as:

$$\begin{aligned} OP_{ipSIC} &= [F_{|Z|^2}(\tau_c)]^L + [F_{|Z|^2}((\omega P_B |h_{irul}|^2 + N_0) \tau_p)]^L \\ &\quad - [F_{|Z|^2}(\min\{\tau_c, (\omega P_B |h_{irul}|^2 + N_0) \tau_p\})]^L \end{aligned} \quad (11)$$

where,

$$\begin{aligned} F_{|Z|^2}(\tau_c) &= \mu \sum_{b=0}^{K-k} \binom{K-k}{b} \frac{(-1)^b}{k+b} \\ &\quad \times \left[1 - \frac{2}{\Gamma(Q)} \left(\frac{\sqrt{\tau_c}}{\sigma^2} \right)^Q K_Q \left(\frac{2\sqrt{\tau_c}}{\sigma^2} \right) \right]^{k+b} \end{aligned} \quad (12)$$

Similarly,

$$\begin{aligned} F_{|Z|^2} &\left((\omega P_B |h_{irul}|^2 + N_0) \tau_p \right) \\ &= \int_0^\infty f_{|h_{irul}|^2}(y) F_{|Z|^2}((\omega P_B y + N_0) \tau_p) dy \\ &= \int_0^\infty \frac{1}{2\sigma_{irul}^2} e^{-\frac{y}{2\sigma_{irul}^2}} \mu \sum_{b=0}^{K-k} \binom{K-k}{b} \\ &\quad \times \frac{(-1)^b}{k+b} \left[1 - \frac{2}{\Gamma(Q)} \left(\frac{\sqrt{(\omega P_B y + N_0) \tau_p}}{\sigma^2} \right)^Q K_Q \left(\frac{2\sqrt{(\omega P_B y + N_0) \tau_p}}{\sigma^2} \right) \right]^{k+b} dy \\ &\approx \mu \sum_{a=1}^A \sum_{b=0}^{K-k} \binom{K-k}{b} \frac{(-1)^b W_a}{k+b} \left[1 - \right. \\ &\quad \left. \frac{2}{\Gamma(Q)} \left(\frac{\sqrt{(2\omega P_B \sigma_{irul}^2 \xi_a + N_0) \tau_p}}{\sigma^2} \right)^Q K_Q \left(\frac{2\sqrt{(2\omega P_B \sigma_{irul}^2 \xi_a + N_0) \tau_p}}{\sigma^2} \right) \right]^{k+b} \end{aligned} \quad (13)$$

where $W_a = \frac{(A!)^2 \xi_a}{[L_{A+1}(\xi_a)]^2}$ is the weight of Gauss-Laguerre quadrature formula, ξ_a is the zero point of Laguerre polynomial $L_A(\xi_a)$, $a = 1, 2, 3, \dots, A$, A is the complexity trade-off accuracy, and when $A \rightarrow \infty$, the above formula takes the equal sign.

In summary, by substituting (12), (13) into (11), formulations for the outage probability in the case of ipSIC is:

$$OP_{ipSIC} = \begin{cases} [F_Z(\tau_c)]^L, & (\omega P_B |h_{irul}|^2 + N_0) \tau_p < \tau_c \\ [F_Z((\omega P_B |h_{irul}|^2 + N_0) \tau_p)]^L, & \text{else} \end{cases} \quad (14)$$

4.1.2 Perfect SIC. Available with Section 4.1.1, ideally, the outage probability expression of the system to achieve perfect SIC is:

$$\begin{aligned} OP_{pSIC} &= [F_Z(\tau_c)]^L + [F_Z(\widehat{\tau}_p)]^L - [F_Z(\min\{\tau_c, \widehat{\tau}_p\})]^L \\ &= \begin{cases} [F_Z(\tau_c)]^L, & \widehat{\tau}_p < \tau_c \\ [F_Z(\widehat{\tau}_p)]^L, & \widehat{\tau}_p > \tau_c \end{cases} \end{aligned} \quad (15)$$

where $\widehat{\tau}_p = N_0 \tau_p$,

$$\begin{aligned} F_Z(\widehat{\tau}_p) &= \mu \sum_{b=0}^{K-k} \binom{K-k}{b} \frac{(-1)^b}{k+b} \\ &\quad \times \left[1 - \frac{2}{\Gamma(Q)} \left(\frac{\sqrt{\widehat{\tau}_p}}{\sigma^2} \right)^Q K_Q \left(\frac{2\sqrt{\widehat{\tau}_p}}{\sigma^2} \right) \right]^{k+b} \end{aligned} \quad (16)$$

4.2. Exact Outage Probability of the NOMA Scheme

To further highlight the superiority of RSMA in terms of system performance, the outage probability of NOMA network under the same system model [14] is analyzed. Correspondingly, the SNR for decoding the k -th user signal by the q -th ($1 \leq q \leq k$) user is expressed as:

$$\tilde{\gamma}_{k \rightarrow q} = \max_{\Psi_l} \frac{\alpha_q P_B |\Psi_l^H D_k h_i|^2}{\sum_{i=q+1}^K \alpha_i P_B |\Psi_l^H D_k h_i|^2 + \omega P_B |h_{irru}|^2 + N_0} \quad (17)$$

The SNR for decoding the signal of the K -th user after performing SIC decoding for the $(K-1)$ -th user and removing its interference is given by:

$$\tilde{\gamma}_K = \max_{\Psi_l} \frac{\alpha_K P_B |\Psi_l^H D_K h_i|^2}{\omega P_B |h_{irru}|^2 + N_0} \quad (18)$$

Therefore, the outage probability of user U_k using the On-Off control scheme is defined as:

$$\begin{aligned} OP_{NOMA} &= \min_q \Pr(\tilde{\gamma}_{k \rightarrow q} < \gamma_{thq}) \\ &= \min_q \Pr\left(\frac{\alpha_q P_B |\Psi_l^H D_k h_i|^2}{\sum_{i=q+1}^K \alpha_i P_B |\Psi_l^H D_k h_i|^2 + \omega P_B |h_{irru}|^2 + N_0} < \gamma_{thq}\right) \\ &\approx \left\{ \mu \sum_{d=1}^D \sum_{b=0}^{K-k} \binom{K-k}{b} \frac{(-1)^b W_d}{k+b} \left[1 - \frac{2}{\Gamma(Q)}\right. \right. \\ &\quad \left. \left. \times \left(\frac{\sqrt{(2\omega P_B \sigma_{irru}^2 \xi_d + N_0) \tau_q}}{\sigma^2}\right)^Q K_Q\left(\frac{2\sqrt{(2\omega P_B \sigma_{irru}^2 \xi_d + N_0) \tau_q}}{\sigma^2}\right)\right] \right\}^{k+b} \quad (19) \end{aligned}$$

where, $\gamma_{thq} = 2^{R_q} - 1$ is the threshold SNR for the q -th user, where R_q is the target data rate for decoding the message, $\tau_q = \frac{\gamma_{thq}}{(\alpha_q - \gamma_{thq} \sum_{i=q+1}^K \alpha_i) P_B}$, and $W_d = \frac{(D!)^2 \xi_d}{[L_{D+1}(\xi_d)]^2}$ is the weight of the Gauss-Laguerre quadrature formula, with ξ_d being the zero point of the Laguerre polynomial $L_D(\xi_d)$.

4.3. Asymptotic Outage Probability of the RSMA Scheme

To further analyze the impact of ipSIC on outage performance, this subsection derives the asymptotic outage probability of the k -th user under high SNR conditions. As $\gamma = \frac{1}{N_0} \rightarrow \infty$, the terms $\{\tau_c, (\omega P_B |h_{irru}|^2 + N_0) \tau_p, \widehat{\tau}_p\} \rightarrow 0$. To simplify the calculation, a series representation of the modified Bessel function $K_\nu(\cdot)$ is used to obtain a high SNR approximation. Specifically, when $\nu = 1$ and $\nu \geq 2$, $K_\nu(\cdot)$ can be approximated as:

$$K_1(x) \approx \frac{1}{x} + \frac{x}{2} \ln\left(\frac{x}{2}\right) \quad (20)$$

$$K_\nu(x) \approx \frac{1}{2} \left[\frac{2^\nu (v-1)!}{x^\nu} - \frac{2^{\nu-2} (v-2)!}{x^{\nu-2}} \right] \quad (21)$$

Taking the first term of the series expansion ($b=0$) as the dominant term, the asymptotic expressions for $F_{|Z|^2}(\tau_c)$, $F_{|Z|^2}((\omega P_B |h_{irru}|^2 + N_0) \tau_p)$, and $F_{|Z|^2}(\widehat{\tau}_p)$ under high SNR conditions can be computed as:

$$\begin{cases} F_{|Z|^2}^{asy}(\tau_c) = \frac{K!}{(K-k)!k} \left[-\frac{2\tau_c}{\sigma^4} \ln\left(\frac{\sqrt{\tau_c}}{\sigma^2}\right) \right]^k \\ F_{|Z|^2}^{asy}(\widehat{\tau}_p) = \frac{K!}{(K-k)!k} \left[-\frac{2\widehat{\tau}_p}{\sigma^4} \ln\left(\frac{2\sqrt{\widehat{\tau}_p}}{\sigma^2}\right) \right]^k \end{cases} \quad Q=1 \quad (22)$$

$$\begin{cases} F_{|Z|^2}^{asy}(\tau_c) = \frac{K!}{(K-k)!k} \left[\frac{\tau_c}{(Q-1)\sigma^4} \right]^k \\ F_{|Z|^2}^{asy}(\widehat{\tau}_p) = \frac{K!}{(K-k)!k} \left[\frac{\widehat{\tau}_p}{(Q-1)\sigma^4} \right]^k \end{cases} \quad Q \geq 2 \quad (23)$$

$$\begin{aligned} F_{|Z|^2}^{asy}((\omega P_B |h_{irru}|^2 + N_0) \tau_p) &\approx \frac{K!}{(K-k)!k} \sum_{a=1}^A W_a \\ &\times \left[1 - \frac{2}{\Gamma(Q)} \left(\frac{\sqrt{2\omega P_B \sigma_{irru}^2 \xi_a \tau_p}}{\sigma^2} \right)^Q K_Q \left(\frac{2\sqrt{2\omega P_B \sigma_{irru}^2 \xi_a \tau_p}}{\sigma^2} \right) \right]^k \quad (24) \end{aligned}$$

In summary, by substituting equations (22), (23), and (24) into (14) and (15), the asymptotic outage probability expressions for pSIC and ipSIC can be derived as follows:

$$OP_{pSIC}^{asy} = \begin{cases} \left[F_{|Z|^2}^{asy}(\tau_c) \right]^L, \widehat{\tau}_p < \tau_c \\ \left[F_{|Z|^2}^{asy}(\widehat{\tau}_p) \right]^L, \widehat{\tau}_p > \tau_c \end{cases} \quad (25)$$

$$OP_{ipSIC}^{asy} = \begin{cases} \left[F_{|Z|^2}^{asy}(\tau_c) \right]^L, (\omega P_B |h_{irru}|^2 + N_0) \tau_p < \tau_c \\ \left[F_{|Z|^2}^{asy}((\omega P_B |h_{irru}|^2 + N_0) \tau_p) \right]^L, else \end{cases} \quad (26)$$

4.4. Diversity Order

To gain better insights, the diversity order is commonly used to evaluate the outage behavior of a communication system. This metric describes the rate at which the outage probability decreases as the transmitted SNR decreases [15]. Therefore, the diversity order can be expressed as:

$$D = - \lim_{\gamma \rightarrow \infty} \frac{\log(OP^{asy})}{\log \gamma} \quad (27)$$

where $OP^{asy} \in \{OP_{pSIC}^{asy}, OP_{ipSIC}^{asy}\}$.

Remark 1. After substituting equation (25) into (27), the diversity order of the k -th user under pSIC is kL . It can be observed that the diversity order of the k -th user is influenced by the number of RIS reflecting elements and the channel ordering.

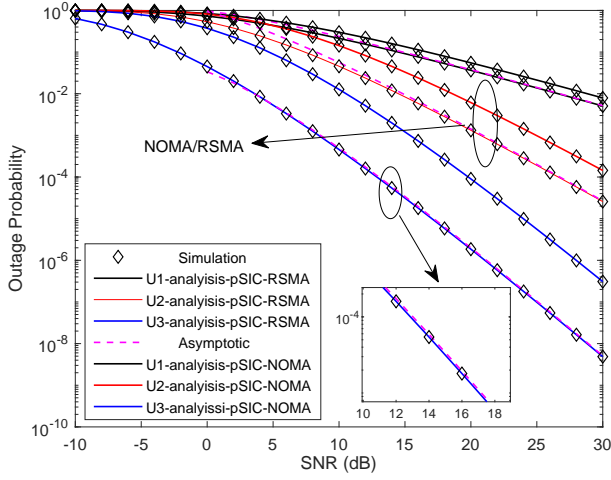


Figure 2. Comparison of Outage Probability for Different Users Using RSMA and NOMA Schemes with pSIC.

Remark 2. When equation (26) is substituted into (27), the diversity order of the k -th user under ipSIC is zero. This is due to the residual interference caused by ipSIC.

5. Numerical and Simulation Results

In this section, numerical simulations are conducted through specific experiments to validate the theoretical analysis presented earlier, investigating the impact of the number of reflective elements in RIS and ipSIC on the system outage performance. Furthermore, to further analyze the performance of the RSMA system, simulation experiments are carried out to evaluate the outage probability of an RIS-assisted multi-user communication system based on NOMA under the same communication model and parameter configurations. The results are then compared with those of the RSMA scheme. The complexity-accuracy tradeoff A and D is set to 5, and the BS transmission power P_B is set to 10dB.

Fig.2 depicts the curves of outage probability versus SNR for three users with pSIC. Set $K = 3, N=1, Q=1$, and $R_c=R_p=R_q=0.45$. It is evident that, throughout the entire average SNR range, the theoretical and simulation outage probability curves almost coincide. The asymptotic outage probability converges to the analytical expression derived in Eq.(20), which confirms the correctness of our theoretical derivation. As observed from the figure, user U3 ($k=3$), which is closer to the BS, exhibits better outage performance compared to U1 and U2. This phenomenon arises because U3 attains a higher diversity order, corroborating the insights presented in **Remark 1**. Moreover, under identical conditions, the RSMA scheme outperforms the NOMA

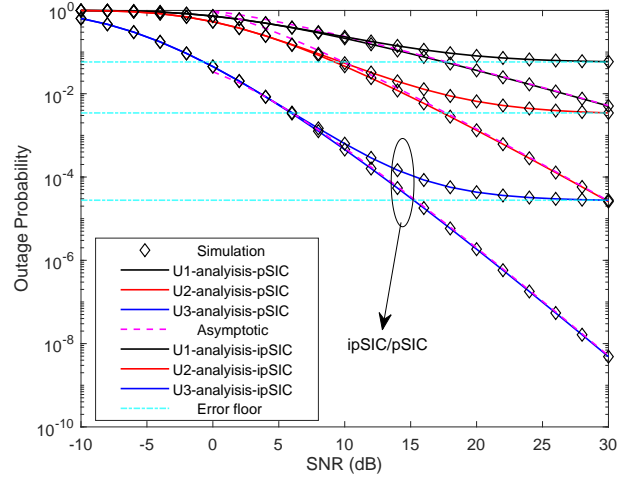


Figure 3. Outage probability versus the transmit SNR with pSIC and ipSIC.

scheme in terms of system outage performance, particularly demonstrating a significant advantage in outage probability at high SNR regimes.

Fig.3 illustrates the relationship between outage probability and SNR for three users in both the pSIC and ipSIC scenarios. Set the rate splitting factor of each user are set to $\alpha_c = 0.4, \alpha_1 = 0.3, \alpha_2 = 0.2, \alpha_3 = 0.1$ respectively and the normalized power of residual interference $E\{|h_{iru}|^2\} = -10dB$. Similar to Fig.2, the theoretical and simulation outage probability curves for the users almost coincide, further validating the accuracy of the theoretical analysis. It is clearly observed from the figure that, throughout the entire SNR range, the outage performance of users in the pSIC scenario consistently outperforms that in the ipSIC scenario. Furthermore, the outage probability of users with ipSIC converges to the error floor at high SNR, indicating that the system's diversity order is zero. This is due to the residual interference generated by ipSIC, which validates the insight presented in **Remark 2**.

Fig.4 plots the relationship between outage probability and SNR for three users, considering different levels of interference caused by ipSIC. The normalized residual interference power is set to $E\{|h_{iru}|^2\} = -10, -8, -7$ dB. From the figure, it can be observed that the outage probability of users decreases as SNR increases. Furthermore, when considering user sorting, users can still achieve better outage performance even in the ipSIC scenario. It is noteworthy that, as the residual interference power increases, the outage probability of IRS-RSMA converges to the worst-case error floor. Therefore, it is crucial to consider the impact of ipSIC on the performance of IRS-NOMA networks in practical

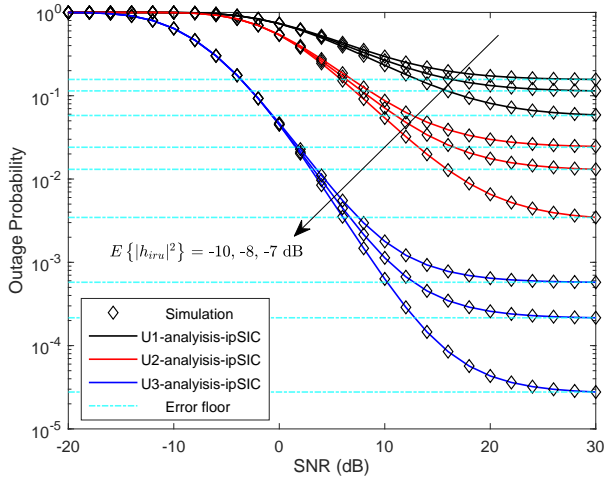


Figure 4. Outage probability of various residual interference power versus the transmit SNR

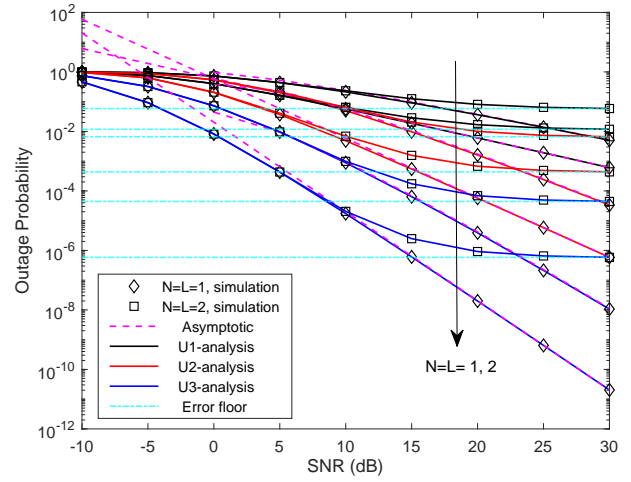


Figure 6. Outage probability of various users versus the transmit SNR with various N and $Q=1$.

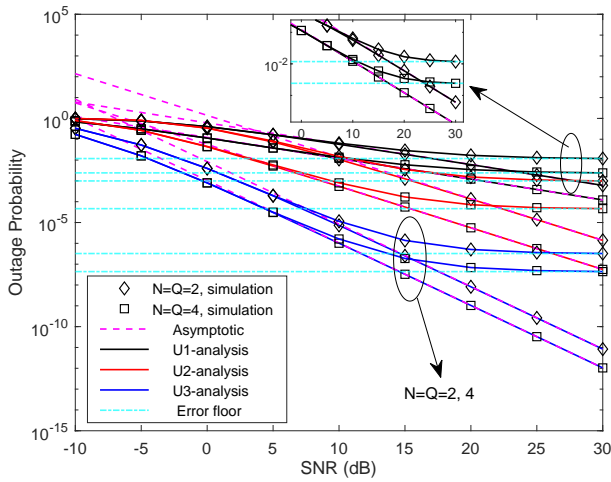


Figure 5. Outage probability of various N versus the transmit SNR with $Q=2$, $L=1$ and $E\{|h_{irsu}|^2\} = -10dB$

scenarios. Similarly, it is equally important to assess the effect of ipSIC on the performance of IRS-RSMA networks in real-world applications.

Fig.5 depicts the curves of interruption probability as a function of SNR for three users under the ipSIC and pSIC scenarios, with different grouping strategies for the number of RIS elements ($Q \geq 2$). It can be observed that the number of RIS reflective elements has a significant impact on network performance. As the number of reflective elements N increases, the interruption probability of users decreases. This is because an increase in the number of RIS elements provides more spatial degrees of freedom. This

phenomenon further validates the effectiveness of **Remark 1**, which states that the number of reflective elements and the user ranking influence the diversity order of users. Additionally, it can be observed that the interruption probability curves of the users exhibit the same slope, indicating that the users share the same diversity order. This observation confirms the analytical results presented in Eq.(23).

Fig.6 illustrates the curves of interruption probability as a function of SNR for three users under the ipSIC and pSIC scenarios, with $Q = 1$ and varying numbers of reflective elements N . The asymptotic interruption probability curves, derived from Eq.(22), are also plotted and show excellent agreement with the simulation results. As observed in the figure, as the number of reflective elements increases, the interruption probability of the users decreases. The main reason behind this is that the RIS, employing the On-Off control scheme, provides more diversity order, as mentioned in **Remark 2**. Notably, the interruption probability curves for each user exhibit different diversity orders, which confirms the analytical results derived in Eq.(22).

6. Conclusion

Although extensive research has been conducted on RIS-assisted communication systems, the outage performance analysis of RIS-assisted RSMA networks in the presence of residual interference remains insufficiently addressed. Most existing studies overlook the impact of effective cascaded channel gains from user ordering and assume ideal continuous phase shifts at the RIS. This paper investigates the outage performance of an RSMA-based communication system

under residual interference, considering a practical RIS model with discrete phase shifts controlled via a switching mechanism. The analysis reveals that both the number of RIS reflecting elements and the level of residual interference significantly affect system performance. While residual interference can degrade communication quality, increasing the number of RIS elements enhances the system diversity gain, effectively mitigating interference and improving outage performance. Furthermore, comparison with RIS-assisted NOMA networks shows that RSMA offers a notable advantage in terms of outage performance.

Appendix A. Proof of Theorem 1

According to [16], the PDF of the Rayleigh cascade channel $|Z|^2$ from BS to RIS to the user is:

$$f_{|Z|^2}(z) = \frac{2\sqrt{z}^{Q-1}}{\Gamma(Q)\sigma^{2(Q+1)}} \cdot K_{Q-1}\left(\frac{2\sqrt{z}}{\sigma^2}\right) \quad (\text{A.1})$$

where $\Gamma(\cdot)$ denotes the Gamma function and $K_\nu(\cdot)$ denotes the second modified Bessel function of order ν .

Based on the above assumptions, the effective cascade channel gain of the RIS auxiliary link using the switching control scheme is sorted to the user: $|\Psi_p^H D_1 g_{i1}|^2 \leq \dots \leq |\Psi_p^H D_k g_{ik}|^2 \leq \dots \leq |\Psi_p^H D_K g_{iK}|^2$. The CDF of the sorted effective cascade channel gain $F_{|Z|^2}(z)$ has a specific correlation with unordered channel gain [7] and [17]:

$$F_{|Z|^2}(z) = \mu \sum_{b=0}^{K-k} \binom{K-k}{b} \frac{(-1)^b}{k+b} [\widehat{F}_{|Z|^2}(z)]^{k+b} \quad (\text{A.2})$$

where $F_{|Z|^2}(z)$ is the cumulative distribution function of the unsorted cascaded channel gain.

From (A.1), the PDF of the unsorted concatenated channel is:

$$\widehat{f}_{|Z|^2}(z) = \frac{2\sqrt{z}^{Q-1}}{\Gamma(Q)\sigma^{2(Q+1)}} K_{Q-1}\left(\frac{2\sqrt{z}}{\sigma^2}\right) \quad (\text{A.3})$$

By integrating the (A.3), the CDF of the unsorted cascaded channel is obtained:

$$\widehat{F}_{|Z|^2}(z) = \frac{2}{\Gamma(Q)\sigma^{2(Q+1)}} \int_0^z x^{\frac{Q-1}{2}} K_{Q-1}\left(\frac{2\sqrt{x}}{\sigma^2}\right) dx \quad (\text{A.4})$$

Let $x = zy$, the Gauss-Laguerre quadrature formula is used for (10):

$$\widehat{F}_{|Z|^2}(z) = 1 - \frac{2}{\Gamma(Q)} \left(\frac{\sqrt{z}}{\sigma^2}\right)^Q K_Q\left(\frac{2\sqrt{z}}{\sigma^2}\right) \quad (\text{A.5})$$

Finally, Eq.(A.5) is substituted into Eq.(A.2), and the CDF of the effective cascade channel after the RIS auxiliary link is sorted is obtained, and the proof is completed.

Acknowledgement

This work was supported by the National Natural Science Foundation of China under Grant 62461032 and 62001359, the Tianyou Youth Talent Lift Program of Lanzhou Jiaotong University, and the Key Research and Development Project of Lanzhou Jiaotong University ZDYF2304.

References

- [1] Liu, Y et al. Evolution of NOMA Toward Next Generation Multiple Access (NGMA) for 6G. *IEEE Journal on Selected Areas in Communications*. 2022; 40(4):1037-1071.
- [2] Li, Z., Yuan, W., Li, B., Wu, J., You, C., Meng, F. Reconfigurable-Intelligent-Surface-Aided OTFS: Transmission Scheme and Channel Estimation. *IEEE Internet of Things Journal*. 2023; 10(22):19518-19532.
- [3] Katwe, M., Singh, K., Clerckx, B., Li, C. -P. Rate-Splitting Multiple Access and Dynamic User Clustering for Sum-Rate Maximization in Multiple RISs-Aided Uplink mmWave System. *IEEE Transactions on Communications*. 2022; 70(11):7365-7383.
- [4] Mao, Y., Dizdar, O., Clerckx, B., Schober, R., Popovski P., Poor, H. V. Rate-Splitting Multiple Access: Fundamentals, Survey, and Future Research Trends. *IEEE Communications Surveys & Tutorials*. 2022; 24(4):2073-2126.
- [5] Sadia, H., Abbas, Z. H., Hassan, A. K., Abbas, G. Outage Probability Analysis of Reconfigurable Intelligent Surface (RIS)-Enabled NOMA Network. In: 10th International Conference on Wireless Networks and Mobile Communications (WINCOM). 2023; pp. 1-6. Istanbul, Turkiye.
- [6] Zheng, B., Wu, Q., Zhang, R. Intelligent Reflecting Surface-Assisted Multiple Access With User Pairing: NOMA or OMA?. *IEEE Communications Letters*. 2020; 24(4):753-757.
- [7] Fu, M., Zhou, Y., Shi, Y. Intelligent Reflecting Surface for Downlink Non-Orthogonal Multiple Access Networks. In: *IEEE Globecom Workshops (GC Wkshps)*. 2019; pp. 1-6. Waikoloa, HI, USA.
- [8] Gu, J., Wang, M., Duan, W., Zhang, L., Zhang, H. Imperfect SIC for NOMA Communications Under Nakagami-m Fading: Comparison of RIS and Relay. In: 20th International Conference on the Design of Reliable Communication Networks (DRCN). 2024; pp. 17-23. Montreal, QC, Canada.
- [9] Hu, J., Liu, G., Ma, Z., Xiao, M., Fan, P. Low-Complexity Resource Allocation for Uplink RSMA in Future 6G Wireless Networks. *IEEE Communications Letters*. 2024; 13(2):565-569.
- [10] Bansal, A., Singh, K., Clerckx, B., Li, C. -P., Alouini, M. -S. Rate-Splitting Multiple Access for Intelligent Reflecting Surface Aided Multi-User Communications. *IEEE Transactions on Vehicular Technology*. 2021; 70(9):9217-9229.
- [11] Yang, Z., Shi, J., Li, Z., Chen, M., Xu, W., Shikh-Bahaei, M. Energy Efficient Rate Splitting Multiple Access (RSMA) with Reconfigurable Intelligent Surface. In: *IEEE International Conference on Communications Workshops (ICC Workshops)*. 2020; pp. 1-6. Dublin, Ireland.

- [12] Ding, Z., Vincent Poor, H. A Simple Design of IRS-NOMA Transmission. *IEEE Communications Letters*. 2020; 24(5):1119-1123.
- [13] Papoulis, A., U. Pillai, S. *Probability, Random Variables, and Stochastic Processes*. 4th edn. McGraw-Hill, New York, NY, USA(2002).
- [14] Yue X., Liu Y. Performance Analysis of Intelligent Reflecting Surface Assisted NOMA Networks. *IEEE Transactions on Wireless Communications*. 2022; 21(4):2623-2636.
- [15] Fernández S., Alfonso Bailón-Martínez J., Galeote-Cazorla J. E., Javier López-Martínez F. Analytical Characterization of the Operational Diversity Order in Fading Channels. *IEEE Communications Letters*. 2025; 29(2):274-278.
- [16] Liu, H., Ding, H., Xiang, L., Yuan, J., Zheng, L. Outage and BER performance analysis of cascade channel in relay networks. *Procedia Computer Science*. 2014; 34(8):23–30.
- [17] Yue, X., Qin, Z., Liu, Y., Kang, S., Chen, Y. A Unified Framework for Non-Orthogonal Multiple Access. *IEEE Transactions on Communications*. 2018; 66(11):5346-5359.